MedChemComm

CONCISE ARTICLE

View Article Online
View Journal | View Issue

Cite this: *Med. Chem. Commun.*, 2014, **5**, 808

Metabolism of a novel skepinone L-like p38 mitogen-activated protein kinase inhibitor

K. Storch, M. Gehringer, B. Baur and S. A. Laufer*

Received 7th March 2014
Accepted 15th April 2014

DOI: 10.1039/c4md00106k

www.rsc.org/medchemcomm

The p38 mitogen-activated protein kinase (MAPK) is a key mediator in cytokine-induced signaling events and is activated in response to a variety of extracellular stimuli such as stress factors, UV-light and inflammatory cytokines. Therefore, the p38 MAP kinase plays an integral role in disease states including oncogenesis, immune disorders and inflammatory processes. Recently a novel class of highly selective p38α inhibitors was described and characterized as tools and probes for *in vivo* studies. The objective of the current study was the preclinical characterization of 3-((2,4-difluorophenyl)amino)dibenzo[*b*,*e*]oxepin-11(6*H*)-one, a potent p38α MAP kinase inhibitor. In rat and human hepatic microsomal incubations, the examined compound is completely inactivated (concerning the inhibitory potency of the isolated p38α enzyme) by a CYP2B6 mediated phase 1 metabolism. The dehalogenation and subsequent hydroxylation in the *para* position of the 2,4-difluorophenyl residue was found to be the predominant transformation. The metabolite was detected in different quantities in both species. In a consecutive reaction the phase 1 metabolite conjugates with glucuronic acid in terms of a phase 2 metabolism. The responsible isoenzymes were identified to be UGT1A3, UGT1A9 and UGT1A10. In this reaction UGT1A10 is the predominant driver of the conversion. Similar to the phase 1 metabolite, the conjugate could also be found in different amounts in both examined species.

Introduction

The p38α kinase is the best-characterized member of the mitogen activated protein kinase (MAPK) family. It plays a central regulatory role in the production of pro-inflammatory cytokines like TNF-α, interleukin-1β, and interleukin-6β.[1] The MAPK family is a group of serine/threonine kinases,[2] which are activated by various extracellular stimuli, such as heat shock, osmotic shock or irradiation with UV light.[3] Once being activated it mediates the signal transduction into the nucleus to turn on responsive genes. Diseases linked to this pathway are rheumatic arthritis,[4,5] COPD, Crohn's disease[6,7] or asthma.[8,9] Consequently, p38 inhibitors have been considered as anti-TNF-α therapeutics that could potentially replace established anti-TNF antibodies or TNF receptors.

Many pharmaceutical companies initiated p38 discovery programs,[10,11] but despite the fact that a few candidates have reached phase III of clinical development, safety issues appear to be the main hurdle for a successful development. Especially when administered at high concentrations, many compounds showed toxic properties.[12–14] Moreover kinase inhibitors are known to change their selectivity profile through metabolic transformations, adding an additional layer of complexity to toxicity prediction.[15]

There are four isoforms of p38 that demonstrate different patterns of tissue expression[16–18] and activation.[16] Several studies show that the α isoform is the major contributor to the role of p38 in inflammation.[19–21] Besides the fact that there is a need for new potent p38 MAP kinase inhibitors showing high efficacy even at low dosage, ADMET investigations become more and more important.

As recently reported by our group,[22] dibenzosuberones are highly selective and potent p38 MAP kinase inhibitors. A prominent example within this inhibitor class is skepinone-L, which has an outstanding potency in an isolated p38 enzyme assay as well as a human whole blood assay measuring the inhibition of TNF-α release. Furthermore, skepinone-L is hardly affected by metabolic conversion and displays favorable pharmacokinetic characteristics.

We also reported,[23] that the metabolism of related dibenzosuberones gets suppressed by the introduction of hydrophilic side chains in position 9 of the A-ring. Besides increasing the hydrophilicity of the molecule, blocking the metabolically labile position of the central scaffold by introducing an ether bridge is the way of choice to prevent metabolic degradation. This concept led to another series of p38 inhibitors based on a dibenzo[*b*,*e*]oxepin-11(6*H*)-one core. Again hydrophilic side chains lead to increased metabolic stability. Based on the recently published results[23] the present study determined that

Eberhard Karls University of Tuebingen, Institute of Pharmaceutical Sciences, Department of Pharmaceutical and Medicinal Chemistry, Auf der Morgenstelle 8, D-72076 Tuebingen, Germany. E-mail: stefan.laufer@uni-tuebingen.de

the main scaffold 3-((2,4-difluorophenyl)amino)dibenzo[*b*,*e*]-oxepin-11(6*H*)-one is metabolized to a single metabolite bearing the corresponding hydroxyl function in *para* position of the 2,4-difluorophenyl moiety. The metabolism of this compound was simulated in rat liver microsomes as well as in human liver microsomes. Its phase 1 metabolism is exclusively mediated by CYP2B6. CYP2B6 is assumed to be expressed at only 3 to 5% of total P450s in human livers.[24,25] Its expression and enzyme activity has been shown to vary approximately 100 fold in the human liver.[26] Cytochrome 2B6 is also expressed in extrahepatic tissues such as brain, kidney, intestine,[24] uterine endometrium,[27] skin,[28] and heart.[29] It is one of the most polymorphic CYP genes in humans and currently 30 defined alleles with over 100 described polymorphisms are known.[30,31] The polymorphic nature of the cytochrome P450 (CYP450) genes affects individual drug response and reactions to a big extent.[32] Studies of human liver tissues have shown that females tend to express higher levels of CYP2B6 in liver than males.[30] In an extension of the phase 1 metabolism study, incubations with glucuronosyltransferases (UGT) were performed. UGTs are responsible for glucuronidation, a major contributor to phase 2 metabolism.[33] Incubations were again performed with rat and human liver microsomes as well as with different UGT isoenzymes. UGT1A3, 1A9 and 1A10 were identified to be involved in this reaction. Each of these three isoenzymes shows a genetic polymorphism in humans.[34–37] Moreover UGT1A10 was identified as the key driver of the conversion.

Results

Metabolic stability of compound 1 in different species: male/female Sprague Dawley rat liver microsomes, and male/female human liver microsomes

The main metabolite of compound **1** was the corresponding 3-((2-fluoro-4-hydroxyphenyl)amino)dibenzo[*b*,*e*]oxepin-11(6*H*)-one. The introduction of a hydroxyl group in *ortho* position to the amino function (substituting the *ortho*-F) was not observed (Fig. 1).

This can primarily be attributed to the lower steric hindrance at the *para* position as well as to electronic factors. By analyzing both possible metabolites by HPLC, a retention time shift was observed between **2a** and **2b** (see Fig. 2). Although both compounds possess the same calculated log *P* value, they differ significantly in lipophilicity. This observation can be explained by reduced solvation of **2b** due to increased steric bulk around the hydroxyl group. Furthermore, a weak intramolecular hydrogen bond[38] between the hydroxy and the diarylamino function can be formed in **2b**, which partially masks the polar groups from hydrogen bonding with the solvent. Moreover, a conformational bias within **2b** caused by this intramolecular hydrogen bond could further alter the lipophilicity of the molecule.

MS/MS data did not provide any further information because both potential metabolites show an almost identical fragmentation pattern. Kinetic analysis demonstrated that the metabolite of compound **1** reached a concentration maximum between 100 and 120 min. The metabolite could be found in different amounts in both human and rat liver microsomes.

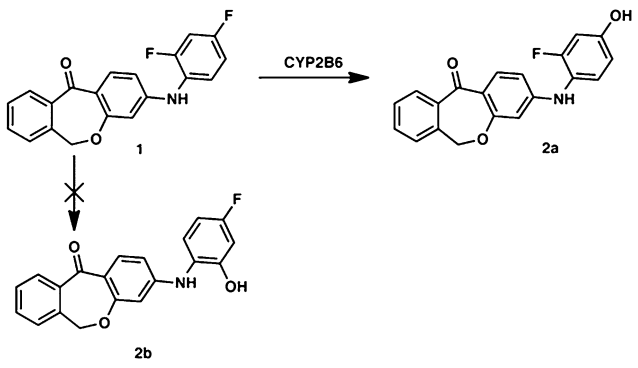

Fig. 1 Metabolic profile of compound **1** with the enzyme involved in the biotransformation. The metabolic pathway was proven in rat and human hepatic microsomes after incubation for 180 min.

In vitro phase 1 metabolism in female and male rat and human liver microsomes

To examine gender-specific differences, incubations with male and female pooled RLMs as well as with male and female pooled HLMs were performed. The time profile of the RLMs showed clear-cut differences in the metabolite formation rates (Table 1). Male RLMs produced the metabolite faster, compared with female RLMs (Fig. 3). In HLMs, gender differences were much less distinct, especially when considering the higher P450 enzyme activity of female microsomes (see Table 1).[30]

In vitro phase 1 metabolism in baculovirus-expressed human P450 isoenzymes

The dehalogenation was catalyzed exclusively by CYP2B6, which was confirmed by incubation with several isolated P450 isoforms (CYP1A2, CYP2A6, CYP2B6, CYP3A4, CYP2C8, CYP2C9, CYP2C19, CYP2D6, CYP2J2, CYP4F12; see Table 2). Negative controls without NADPH and with cytochrome P450 reductase/b5 without P450 enzymes were carried out to exclude non-enzymatic metabolite formation.

Kinetics of phase 1 metabolism

The kinetic parameters K_M and v_{max} were determined by incubating **1** (1–200 μM) with male and female HLM (0.19 mg mL^{-1}), male/female RLM (0.15 mg mL^{-1}) as well as with rCYP2B6 (0.1 mg mL^{-1}). Calculated K_M and v_{max} values are shown in Table 2. The respective Michaelis–Menten (M–M) plots of compound **1** can be found in Fig. 4. The M–M plots show a hyperbolic curve, indicating saturation of the metabolite formation over the substrate range used suggesting that the data obeyed M–M kinetics. M–M values did not differ significantly between male and female HLMs (see Table 2).

In vitro phase 2 metabolism in baculovirus-expressed human UGT isoforms

In order to identify the isoenzymes responsible for the glucuronidation, incubations with a set of different UGT isoforms

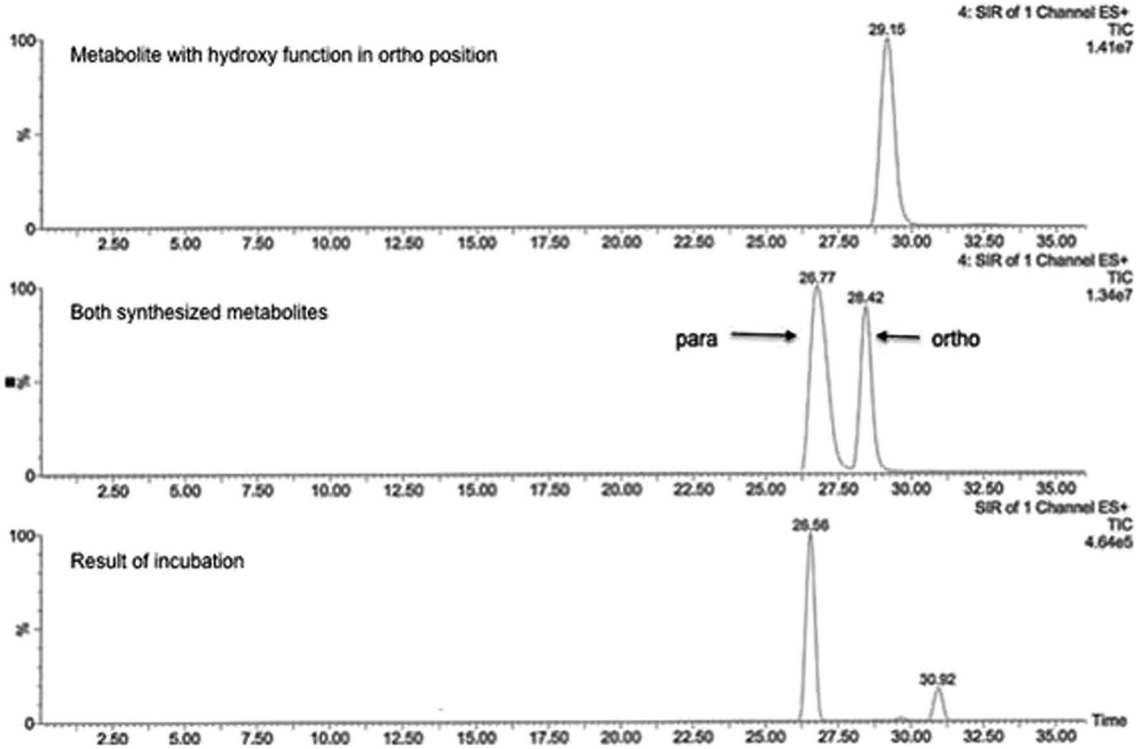

Fig. 2 Representative chromatogram showing the feasibility of metabolite separation. The analysis was performed on RP-HPLC system with mass selective detection (positive ESI mode, SRM detection).

Table 1 Phase 1 metabolite formation of compound **1** in different species and CYP isoenzymes. Incubations were performed for 180 min and aliquots were taken at predefined time points. After protein degradation and centrifugation the supernatant was directly used for LC-MS analysis

Species	Gender specifity	$t_{1/2}$ [min]
Human	Male	21.40 ± 2.43
	Female	44.81 ± 8.54
Rat	Male	23.63 ± 2.71
	Female	41.70 ± 8.86
CYP2B6[a]		14.36 ± 0.09

[a] Incubations with the other isoforms did not show any conversion.

(UGT1A1, UGT1A3, UGT1A6, UGT1A7, UGT1A9, UGT1A10, UGT2B7, UGT2B15) were performed. The conjugation of **2a** with glucuronic acid was mediated by UGT1A3, UGT1A9 and UGT1A10. The latter was identified to play a dominant role in the conversion (see Fig. 5). Incubations without UDPGA were used to rule out non-enzymatic conversion.

In vitro phase 2 metabolism in pooled rat and male/female human liver microsomes.

The time profile of the RLMs showed rapid conversion into the metabolite **3** ($t_{1/2}$ = 9.218 ± 0.81 min). To examine gender-specific differences, incubations of male and female HLMs were compared. Female HLMs ($t_{1/2}$ = 63.02 ± 3.47 min) and male HLMs ($t_{1/2}$ = 65.68 ± 4.78 min) produce the metabolite with no significant difference in formation rates (Fig. 5 and Table 3).

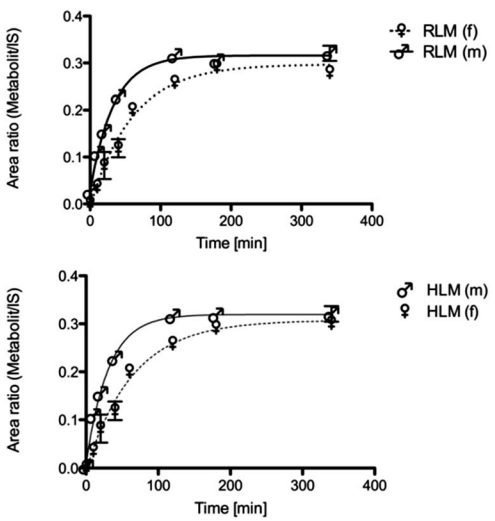

Fig. 3 Metabolic conversion rate of male and female rat liver microsomes in the phase 1 reaction.

Discussion

The cytochrome P450 enzyme system plays a major role for the pharmacokinetics and toxicity of drugs. Knowledge about the dominant cytochrome P450 isoform responsible for the

Table 2 Michaelis–Menten parameters of **1** by product formation

Species	Gender specifity	K_M [μM]	v_{max} [nM min^{-1} per mg protein]	CL_{int} [μL min^{-1} pmol P450]
Human	Male	56.10 ± 12.46	3.015 ± 0.2955	20.19
Human	Female	58.91 ± 10.99	4.562 ± 0.3486	15
Rat	Pooled	63.99 ± 16.89	5.487 ± 0.7227	4.69
rCYP2B6		14.14 ± 4.552	0.6293 ± 0.06293	12.21

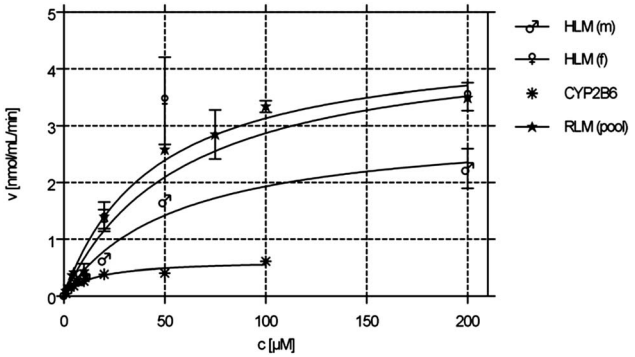

Fig. 4 Michaelis–Menten kinetics (phase 1 metabolism) of male and female HLMs, pooled RLM as well as CYP2B6.

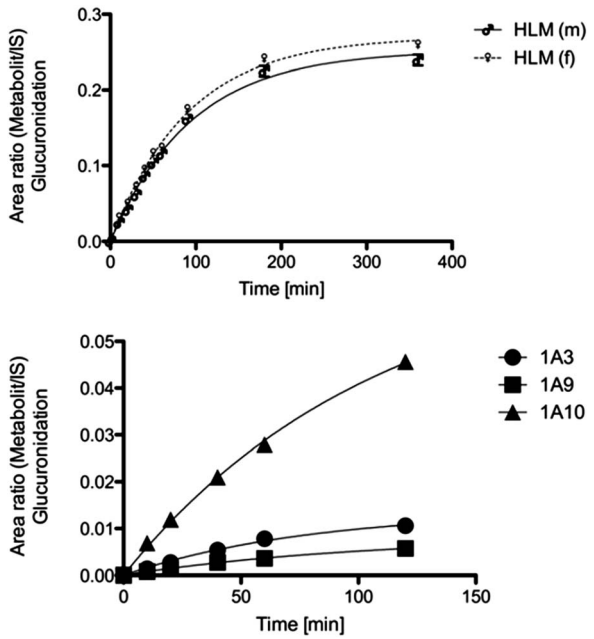

Fig. 5 Metabolic conversion rate of male/female HLMs and recombinant isoenzymes in the phase 2 reaction.

metabolism of a particular drug is valuable in predicting factors like efficacy or potential drug interactions.

For this reason the aim of this study was to investigate the *in vitro* metabolism of 3-((2,4-difluorophenyl)amino)dibenzo[*b*,*e*]-oxepin-11(6*H*)-one, a potent and selective skepinone-L like p38α MAPK inhibitor, by human and rat liver microsomes as cytochrome P-450 enzyme source. Isoenzyme CYP2B6 was identified

Table 3 Phase 2 metabolite formation in different species. Only metabolically active UGT isoforms are listed

Species	Gender specifity	$t_{1/2}$ [min]
Human	Male	65.68 ± 4.78
	Female	63.02 ± 3.47
Rat	Pool	9.218 ± 0.81
UGT1A3		54.92 ± 8.07
UGT1A9		74.67 ± 8.71
UGT1A10		75.36 ± 13.09

as key driver in the phase 1 metabolism of **1**. The value of v_{max} fits into the range between 1 and 15 nmol of product per minute per milligram of microsomal protein, which is in the typically observed range for organic substrates metabolized by cytochrome P-450 enzymes.[39,40] CYP2B6 is mediating the dehalogenation and hydroxylation of the fluorine atom in the *para* position of the difluorphenyl moiety. Through this phase 1 metabolism, compound **1** undergoes a complete inactivation with regard to the inhibition of the isolated p38α enzyme (0.234 μM for substance **1** and 3.293 μM for substance **2b**, respectively). The introduction of a hydroxyl group opens up the opportunity for phase 2 reactions. Phase 2 metabolism was investigated by incubations with uridine 5′-diphosphoglucuronic acid trisodium salt, which revealed a conjugation with glucuronic acid. The conversion was mediated by UGT1A3, UGT1A9 and UGT1A10 with a preference for the latter.

Experimental

Reagents

1: 3-((2,4-difluorophenyl)amino)dibenzo[*b*,*e*]oxepin-11(6*H*)-one, **2a:** 3-((2-fluoro-4-hydroxyphenyl)amino)dibenzo[*b*,*e*]oxepin-11(6*H*)-one, **2b:** 3-((2-hydroxy-4-fluorophenyl)amino)dibenzo[*b*,*e*]oxepin-11(6*H*)-one, the internal standard skepinone-L (**3**) (*R*)-2-((2,4-difluorophenyl)amino)-7-(2,3-dihydroxypropoxy)-10,11-dihydro-5*H*-dibenzo[*a*,*d*][7]annulen-5-one[22] and the corresponding phase 2 metabolite were prepared at the Department of Pharmaceutical and Medicinal Chemistry, University of Tuebingen (Tuebingen, Germany). The corresponding chemical structures are shown in Fig. 6. Acetonitrile (ACN; LC-MS Grade) and methanol (LiChrosolv hypergrade) were purchased from VWR (Darmstadt, Germany). Formic acid (FA) p.a., $NADP^+$ sodium salt, Trizma base and Trizma HCl, magnesium chloride hexahydrate, glucose 6-phosphate sodium salt, and glucose 6-phosphate dehydrogenase from yeast, uridine 5′-diphosphoglucuronic acid

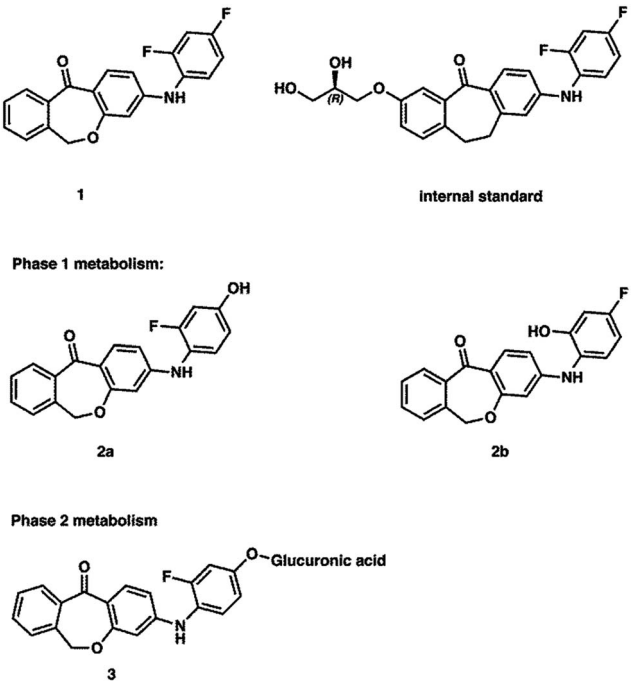

Fig. 6 Chemical structures of all compounds with corresponding IUPAC nomenclature. **1**: 3-((2,4-difluorophenyl)amino)dibenzo[*b*,*e*]oxepin-11(6*H*)-one; **2a**: 3-((2-fluoro-4-hydroxyphenyl)amino)dibenzo[*b*,*e*]oxepin-11(6*H*)-one; **2b**: 3-((4-fluoro-2-hydroxyphenyl)amino)dibenzo[*b*,*e*]oxepin-11(6*H*)-one; **3**: (2*R*,3*R*,4*R*,5*S*,6*R*)-6-(3-fluoro-4-((11-oxo-6,11-dihydrodibenzo[*b*,*e*]oxepin-3-yl)amino)phenoxy)-3,4,5-trihydroxytetrahydro-2*H*-pyran-2-carboxylic acid; internal standard: (*R*)-2-((2,4-difluorophenyl)amino)-7-(2,3-dihydroxypropoxy)-10,11-dihydro-5*H*-dibenzo[*a*,*d*][7]annulen-5-one.

trisodium salt, D-saccharic acid 1,4-lactone monohydrate and alamethicin from *Trichoderma viride* were purchased from Sigma-Aldrich Chemie GmbH (Munich, Germany). Water was obtained from an in-house bi-distillation device (Department of Pharmaceutical and Medicinal Chemistry, University of Tuebingen, Germany).

In vitro metabolism studies (phase 1)

Pooled male and female liver microsomes of rats (RLMs) and humans (HLMs) were purchased from Life Technologies GmbH (Darmstadt, Germany). To compare the rates of substrate degradation, the microsomal protein content was arbitrarily standardized to 1 mg mL^{-1}. All incubations were performed under the same conditions with respect to their protein content.

All incubations (final total volume 1050 μL) were made in the presence of an NADPH-regenerating system consisting of 5 mM glucose 6-phosphate, 5 U mL^{-1} glucose 6-phosphate dehydrogenase, and 1 mM $NADP^+$. The substrate (10 μM), NADPH regenerating system, and 3.8 mM $MgCl_2$ $x6 \cdot H_2O$ in 0.1 M Tris buffer (pH 7.4 at RT) were pre-incubated for 5 min in a shaking heating block at 37 °C, 550 rpm, and the reaction was started by addition of the respective microsomes. To follow the course of metabolism, 100 μL aliquots were withdrawn at different time points (0, 10, 20, 40, 60, 120 and 180 min) and transferred into an ice-cooled vial containing 100 μL internal Standard (100 μg mL^{-1} **3** in acetonitrile, final concentration of 50 μg mL^{-1}). The samples were vortexed for 15 s and centrifuged (19 800 relative centrifugal force/4 °C per 10 min). The supernatant was directly used for analysis. All incubations were conducted in triplicate; average mean values of these incubations are shown in the figures. In all incubations a limit of 1% organic solvent was not exceeded.[41,42]

In vitro metabolism in baculovirus-insect cell expressed human P450 isoenzymes

All isoenzymes (CYP1A2, CYP2A6, CYP2B6, CYP3A4, CYP2C8, CYP2C9, CYP2C19, CYP2D6, CYP2J2, CYP4F12) were purchased from BD Biosciences (Heidelberg, Germany). The final enzyme concentration was 100 pmol mL^{-1} in all incubations. Incubations were conducted according to the liver microsome procedure.

Proof of linearity for protein content and time of incubation

1 was incubated for 90 min with the same protein content in each of the different species' liver microsomes. Five aliquots were drawn at time points 0, 10, 30, 60, and 90 min as described above. The concentration of **1** was set to 100% at $t = 0$ min. The logarithm of the percentage remaining *versus* time was fitted by least-squares linear regression of at least four time points. Goodness of fit was assessed by calculation of the correlation coefficient (R^2) and visual examination of the data.

Determination of kinetic parameters for the dehalogenation of 1 to 2

K_m and v_{max} were determined in pooled female and male human liver microsomes, using baculovirus cDNA-expressed isoenzymes (Supersomes) of CYP2B6 with P450 reductase. The substrate concentrations ranged from 0.1 μM to 50 μM. The protein content and time linearity were proven in the preceding analysis. The protein content determined was 0.03 mg mL^{-1} for HLMs and the cytochrome P450 content was 0.5 pmol mL^{-1} for CYP2B6. Incubations were conducted in a total volume of 250 μL for an incubation time of 10 min, and were performed in triplicate for the liver microsomes and CYP2B6. Data reported are averages ± standard errors of the determinations. Estimation of the enzyme kinetic parameters was made by fitting to the Michaelis–Menten equation by best-fit nonlinear regression using the Enzyme Kinetics Module of the GraphPad Prism software, version 5.0a for Mac OsX (GraphPad Software, San Diego, California, USA, http://www.graphpad.com). Goodness of fit was assessed by calculation of the correlation coefficient (R^2) and visual examination of the data.

In vitro metabolism studies (phase 2)

Phase 2 incubations were performed in analogous manner to phase 1 incubations. The NADPH regenerating system was replaced with uridine 5′-diphosphoglucuronic acid trisodium salt (100 mM), D-saccharic acid 1,4-lactone monohydrate

(100 mM)[43] and alamethicin (100 mM).[44] The workup was done as described in the section above.

Screening of metabolites by LC-MS/MS analysis

Metabolite formation was analyzed with a Jasco (Groβ-Umstadt, Germany) HPLC system consisting of a pump (PU-1580) and an autosampler from CTCAnalytics (HTSPal; Zwingen, Switzerland). The chromatographic separation was performed on a waters symmetry C18 column (150 × 4.6 mm; 5 μm) with a pre-column made of the same material. The injection volume was 30 μL. A binary gradient of 30 min with solvent A (H_2O/ACN/FA; 90/10/0.1%) and solvent B (ACN/0.1% FA) was set to a flow rate of 300 μL min^{-1}. The initial composition of 0% B was held for 3 min, followed by a linear gradient up to 95% B in 20 min, holding for 5 min, changing to 0% B in 1.5 min, and re-equilibrating at the end. The detection was performed on a Micromass Quattro micro triple quadrupole mass spectrometer (Waters GmbH, Eschbronn, Germany) in the electrospray ionization-positive SRM mode. Spray voltage was set to 2.9 kV and the heated capillary operated at 350 °C. The desolvation gas flow worked at 200 L h^{-1}. Eluates from the first 15 min and the last 4 min were diverted to waste in order to prevent contamination of the source due to matrix components. Fig. 7 shows a representative HPLC chromatogram of this metabolism assay. The retention times for compound **1** and the developing metabolite were 30.92 and 26.51 min, respectively, in a 33 min HPLC run (Fig. 7). Metabolites were also identified by direct injection of the according reference material. Substrates and metabolites were quantified by internal standards as well as with calibration curves constructed from known concentrations of reference material.

Data analysis

Enzyme kinetic parameters K_M and v_{max} were determined using nonlinear regression analysis with GraphPad Prism software, version 5.0a for Mac OsX (GraphPad Software, San Diego, California, USA, http://www.graphpad.com). The results are expressed as the mean value of three experiments (±SEM). The concentrations were determined in μmol L^{-1}.

Metabolite formation was analyzed using a one-phase association equation. The half-time was computed as $\ln(2)/K$, where K is the rate constant, expressed in reciprocals of time units.

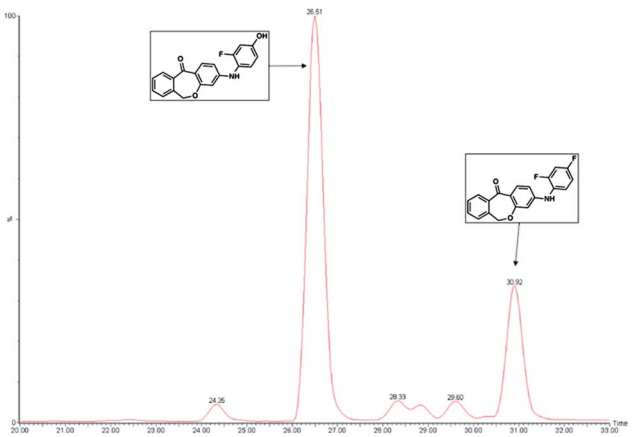

Fig. 7 A representative HPLC chromatogram of phase 1 incubations showing the only metabolite detected in RLMs. Compound **1** (10 μM) was incubated with 1 mg mL^{-1} RLMs for 120 min. **1** and the corresponding metabolite peaks were detected at retention times of 30.92 and 26.51 min, respectively, in a 33 min HPLC run. The peaks in front of the metabolite and between the two observed peaks were determined to be impurities stemming from the RLMs.

Biological testing

The effect of both synthesized compounds on p38α inhibition was tested in an isolated p38α MAP kinase assay. In our system[45] the tested compound competes with adenosine triphosphate (ATP) for the ATP binding site in the catalytic domain. The phosphorylation of activating transcription factor-2 (ATF-2) is determined with an anti-phospho-ATF-2 antibody. The degree of phosphorylation inversely correlates with the inhibitory activity of the tested compounds[46] and was measured using an enzyme-linked immunosorbent assay (ELISA).

Experimental procedures

All commercially available reagents and solvents were used without further purification. ^{1}H NMR (200/400 MHz) and ^{13}C NMR (50/100 MHz) spectra were recorded on a Bruker Advance 200/400 NMR spectrometer. Chemical shifts (δ) are reported in ppm relative to TMS and spectra were calibrated using the solvent resonance. Flash chromatography was performed using an Interchim PuriFlash 430 automated flash chromatography system with self-packed columns containing Davisil LC60A 20-45 micron silica from Grace Davison. The purity of the final compounds was determined by HPLC (Hewlett Packard HP 1090 Series II) LC equipped with a UV diode array detector (DAD, detection at 254 nm). The chromatographic separation was performed on a Phenomenex Luna 5u C8 column (150 mm × 4.6 mm, 5 μm) at 35 °C oven temperature, employing a gradient of 0.01 M KH_2PO_4 (pH 2.3) and methanol as solvent system with a flow rate of 1.0 mL min^{-1}. EI mass spectra were measured on a Hewlett Packard HP 6890 Series GC-MS-system equipped with a HP-5MS capillary column (0.25 EM film thickness 30 m × 0.25 mm) and a Hewlett Packard HP 5973 Mass selective detector (70 eV). FAB (fast atom bombardment) data were obtained from the department for mass spectrometry, Institute of Organic Chemistry, Eberhard-Karls-University Tuebingen. All compounds were >95% pure.

Synthesis of 2b. The synthesis of the dibenzoxepinone core scaffold was performed as described in ref. 47.

Synthesis of 4-fluoro-2-(methoxymethoxy)-1-nitrobenzene. Under argon, 5-fluoro-2-nitrophenol (2.00 g, 12.7 mmol) was dissolved in 75 mL of dry THF and the solution was cooled in an ice bath. Sodium hydride (60% dispersion mineral oil, 559 mg, 14.0 mmol) was added to the solution in one portion. The mixture was slowly warmed to ambient temperature and methoxymethyl chloride (2.1 M solution in toluene, 6.06 mL, 14 mmol) was added dropwise *via* cannula. The mixture was stirred for 3 hours at ambient temperature before quenching with an excess of saturated ammonium chloride solution. The product was extracted with methylen chloride (3 × 100 mL) and the

combined organic layers dried over sodium sulfate. After solvent evaporation, the product was purified by column chromatography (silica gel, gradient 100% petroleum ether to 100% ethyl acetate) to obtain a colorless oil (1.90 g, 12.0 mmol, 94.3%). EI-MS: *m*/*z* 201.1 $[M]^+$, HPLC: 100% (254 nm), ^{1}H NMR (200 MHz, chloroform-*d*) δ_H 7.99–7.81 (1H, m), 7.13–6.98 (1H, m), 6.88–6.67 (1H, m), 5.30 (2H, s), 3.54 (3H, s). ^{13}C NMR (50 MHz, chloroform-*d*) δ_C 165.47 (d, $J_1 = 255.6$ Hz), 152.74 (d, $J_3 = 11.5$ Hz), 128.72 (d, $J_4 = 40.6$ Hz), 127.73 (d, $J_3 = 10.9$ Hz), 108.73 (d, $J_2 = 23.5$ Hz), 104.96 (d, $J_2 = 26.7$ Hz), 95.56, 56.94.

Synthesis of 4-fluoro-2-(methoxymethoxy)aniline. 4-Fluoro-2-(methoxymethoxy)-1-nitrobenzene (1.00 g, 4.97 mmol) was dissolved in 20 mL of ethyl acetate and 10% palladium on carbon (100 mg, 10% wt) was added. Hydrogen was bubbled through the suspension during 5 minutes and the mixture was stirred under hydrogen atmosphere (balloon, ambient temperature) for 8 hours. The mixture was filtered through a pad of celite and the catalyst washed with 100 mL of ethyl acetate. Solvent evaporation gave the pure product as a slightly red oil (844 mg, 4.93 mmol 99.2%). EI-MS: *m*/*z* 171.1 $[M]^+$, HPLC: 95.4% (254 nm), ^{1}H NMR (200 MHz, chloroform-*d*) δ_H 6.83 (1H, dd, $J_{3,4} = 10.2$, 2.6 Hz), 6.74–6.44 (2H, m), 5.18 (2H, s), 3.58 (2H, s), 3.49 (3H, s). ^{13}C NMR (50 MHz, chloroform-*d*) δ_C 156.17 (d, $J_1 = 236.1$ Hz), 145.20 (d, $J_3 = 9.9$ Hz), 132.80 (d, $J_4 = 2.7$ Hz), 115.34 (d, $J_3 = 9.0$ Hz), 108.28 (d, $J_2 = 22.1$ Hz), 103.11 (d, $J_2 = 26.5$ Hz), 95.28, 56.26.

Synthesis of 3-(4-fluoro-2-(methoxymethoxy)amino)-6*H*-dibenzo[*b*,*e*]oxepine-11-one. 3-Chlorodibenzo[*b*,*e*]oxepine-11(6*H*)-one (100 mg, 409 μmol), 4-Fluoro-2-(methoxymethoxy) aniline (77.0 mg, 450 μmol) and cesium carbonate (400 mg, 1.23 mmol) were weighted into a Schlenk tube. The tube was evacuated and backfilled with argon before adding 3 mL of degased dioxane (3 mL). Palladium acetate (4.59 mg, 20.5 μmol) and Xphos (29.2 mg, 61.3 μmol) were added, the tube was sealed and stirred at 80 °C oil bath temperature during 2.5 hours. The reaction was quenched with water and the product extracted with methylen chloride (3 × 50 mL). The combined organic layers were dried over sodium sulfate, the solvent evaporated and the product purified by column chromatography (silica gel, petroleum ether–ethyl acetate 4 : 1). The product was obtained as a yellowish foam (134 mg, 353 μmol, 86.2%). FAB-MS: *m*/*z* 380.2 $[M + H]^+$, HPLC: 100% (254 nm), ^{1}H NMR (200 MHz, chloroform-*d*) δ_H 8.18 (1H, d, $J_3 = 8.9$ Hz), 7.94 (1H, dd, $J_{3,4} = 7.3$, 1.5 Hz), 7.47 (2H, pd, $J_{3,4} = 7.4$, 1.6 Hz), 7.37–7.17 (2H, m), 6.96 (1H, dd, $J_{3,4} = 10.1$, 2.8 Hz), 6.68 (2H, m), 6.54 (1H, d, $J_4 = 2.3$ Hz), 6.26 (1H, s), 5.32–4.97 (4H, m), 3.45 (3H, s). ^{13}C NMR (50 MHz, chloroform-*d*) δ_C 188.64, 163.40, 159.17 (d, $J_1 = 242.9$ Hz), 150.92, 149.70 (d, $J_3 = 10.3$ Hz), 140.70, 135.65, 134.14, 132.25, 129.67, 129.17, 127.68, 126.18 (d, $J_4 = 3.3$ Hz), 122.03 (d, $J_3 = 9.6$ Hz), 118.04, 110.83, 108.35 (d, $J_2 = 22.3$ Hz), 103.65 (d, $J_2 = 26.8$ Hz), 103.01, 95.32, 73.71, 56.50.

Synthesis of 3-(4-fluoro-2-hydroxyphenylamino)-6*H*-dibenzo[*b*,*e*]oxepine-11-one (2b). 3-(4-Fluoro-2-(methoxymethoxy)-amino)-6*H*-dibenzo[*b*,*e*]oxepine-11-one (29.0 mg; 76.4 μmol) were dissolved in a mixture of 7 mL of THF and 7 mL of 10% aqueous HCl. The solution was stirred for 15 h at ambient temperature and the reaction was quenched with saturated $NaHCO_3$ solution (20 mL). The layers were separated and the aqueous layer extracted with ethyl acetate (4 × 30 mL). The combined organic layers were dried over sodium sulfate, the solvent was evaporated and the product purified by gradient column chromatography (silica gel, gradient 100% petroleum ether to 100% ethyl acetate). A yellow foam was obtained (15.4 mg, 49.5 μmol, 60.1%). ESI-MS: *m*/*z* 335.1 $[M + H]^+$, HPLC: 97.4% (254 nm), ^{1}H NMR (200 MHz, chloroform-*d*) δ_H 8.13 (1H, d, $J_3 = 8.9$ Hz), 7.91 (1H, dd, $J_{3,4} = 7.4$, 1.6 Hz), 7.64–7.37 (2H, m), 7.30 (1H, dd, $J_{3,4} = 7.1$, 1.5 Hz), 7.14 (1H, dd, $J_{3,4} = 8.7$, 5.9 Hz), 6.76 (1H, dd, $J_{3,4} = 9.6$, 2.7 Hz), 6.70–6.42 (3H, m), 6.20 (1H, d, $J_4 = 2.0$ Hz), 5.71 (1H, s), 5.10 (2H, s). ^{13}C NMR (50 MHz, chloroform-*d*) δ_C 189.24, 163.55, 159.42, 153.22 (d, $J_3 = 12.6$ Hz), 152.78, 140.64, 135.62, 134.40, 132.47, 129.68, 129.30, 127.82 (d, $J_3 = 10.0$ Hz), 127.78, 120.43 (d, $J_1 = 219.5$ Hz), 110.26, 107.88 (d, $J_2 = 22.8$ Hz), 103.81 (d, $J_2 = 25.7$ Hz), 103.04, 73.79.

Conclusions

Both activity and selectivity of protein kinase inhibitors might be altered by metabolism. The metabolites of oxepine analogs of skepinone-type p38 MAPK-inhibitors are inactive for both p38 and a broad range of other kinases as well (Novartis kinase Panel, data not shown). The metabolic lability of aromatic fluorine residues is another major finding. 2,4-Difluorophenyl residues were hydroxylated to 2-fluoro-4-hydroxyphenyl derivates by CYP2B6.

Acknowledgements

Dr Benjamin Baur and Matthias Gehringer from University of Tuebingen, Department of Pharmaceutical and Medicinal Chemistry designed and executed the synthesis of both possible hydroxyl metabolites. Prof. Dr Stefan Laufer supervised the project and was decisively involved in the initial hypothesis generation as well as in all data discussions and analysis. Kirsten Storch planed, established and accomplished the experimental setup. Moreover she generated/analyzed the data and wrote the manuscript. We thank Novartis Pharma AG (Jörg Trappe, Peter Drückes and Jürgen Köppler) for screening in the Novartis Kinase Panel.

Notes and references

1 J. Lisnock, A. Tebben, B. Frantz, E. A. O'Neill, G. Croft, S. J. O'Keefe, B. Li, C. Hacker, S. De Laszlo, A. Smith, B. Libby, N. Liverton, J. Hermes and P. LoGrasso, *Biochemistry*, 1998, **37**, 16573–16581.
2 K. F. Chung, *Chest*, 2011, **139**, 1470–1479.
3 N. C. Newton and C. P. Decicco, *J. Med. Chem.*, 1999, **42**, 2295–2314.
4 F. Berenbaum, *Curr. Opin. Rheumatol.*, 2004, **16**, 616–622.
5 C. Peifer, G. Wagner and S. Laufer, *Curr. Top. Med. Chem.*, 2006, **6**, 113–149.
6 Y. J. Feng and Y. Y. Li, *J. Dig. Dis.*, 2011, **12**, 327–332.

7 D. Hommes, B. Van Den Blink, T. Plasse, J. Bartelsman, C. Xu, B. Macpherson, G. Tytgat, M. Peppelenbosch and S. Van Deventer, *Gastroenterol*, 2002, **122**, 7–14.
8 R. Newton and N. Holden, *BioDrugs*, 2003, **17**, 113–129.
9 P. J. Barnes, *Discov. Med.*, 2004, **4**, 421–426.
10 J. Hynes Jr and K. Leftheri, *Curr. Top. Med. Chem.*, 2005, **5**, 967–985.
11 S. R. Natarajan and J. B. Doherty, *Curr. Top. Med. Chem.*, 2005, **5**, 987–1003.
12 S. B. Cohen, T.-T. Cheng, V. Chindalore, N. Damjanov, R. Burgos-Vargas, P. DeLora, K. Zimany, H. Travers and J. P. Caulfield, *Arthritis Rheuma*, 2009, **60**, 335–344.
13 R. J. Hill, K. Dabbagh, D. Phippard, C. Li, R. T. Suttmann, M. Welch, E. Papp, K. W. Song, K.-C. Chang, D. Leaffer, Y.-N. Kim, R. T. Roberts, T. S. Zabka, D. Aud, J. Dal Porto, A. M. Manning, S. L. Peng, D. M. Goldstein and B. R. Wong, *J. Pharmacol. Exp. Ther.*, 2008, **327**, 610–619.
14 C. Dominguez, D. A. Powers and N. Tamayo, *Curr. Opin. Drug Discovery Dev.*, 2005, **8**, 421–430.
15 M. W. Karaman, S. Herrgard, D. K. Treiber, P. Gallant, C. E. Atteridge, B. T. Campbell, K. W. Chan, P. Ciceri, M. I. Davis, P. T. Edeen, R. Faraoni, M. Floyd, J. P. Hunt, D. J. Lockhart, Z. V. Milanov, M. J. Morrison, G. Pallares, H. K. Patel, S. Pritchard, L. M. Wodicka and P. P. Zarrinkar, *Nat. Biotechnol.*, 2008, **26**, 127–132.
16 G. Alonso, C. Ambrosino, M. Jones and A. R. Nebreda, *J. Biol. Chem.*, 2000, **275**, 40641–40648.
17 N. W. Court, C. G. dos Remedios, J. Cordell and M. A. Bogoyevitch, *J. Mol. Cell. Cardiol.*, 2002, **34**, 413–426.
18 K. K. Hale, D. Trollinger, M. Rihanek and C. L. Manthey, *J. Immunol.*, 1999, **162**, 4246–4252.
19 J. S. Mudgett, J. Ding, L. Guh-Siesel, N. A. Chartrain, L. Yang, S. Gopal and M. M. Shen, *Proc. Natl. Acad. Sci. U. S. A.*, 2000, **97**, 10454–10459.
20 M. Allen, L. Svensson, M. Roach, J. Hambor, J. McNeish and C. A. Gabel, *J. Exp. Med.*, 2000, **191**, 859–870.
21 V. A. Beardmore, H. J. Hinton, C. Eftychi, M. Apostolaki, M. Armaka, J. Darragh, J. McIlrath, J. M. Carr, L. J. Armit, C. Clacher, L. Malone, G. Kollias and J. S. C. Arthur, *Mol. Cell. Biol.*, 2005, **25**, 10454–10464.
22 S. C. Koeberle, J. Romir, S. Fischer, A. Koeberle, V. Schattel, W. Albrecht, C. Gruetter, O. Werz, D. Rauh, T. Stehle and S. A. Laufer, *Nat. Chem. Biol.*, 2012, **8**, 141–143.
23 B. Baur, K. Storch, K. E. Martz, M. I. Goettert, A. Richters, D. Rauh and S. A. Laufer, *J. Med. Chem.*, 2013, **56**, 8561–8578.
24 L. Gervot, B. Rochat, J. C. Gautier, F. Bohnenstengel, H. Kroemer, V. De Berardinis, H. Martin, P. Beaune and I. De Waziers, *Pharmacogenetics*, 1999, **9**, 295–306.
25 T. Lang, K. Klein, J. Fischer, A. K. Nussler, P. Neuhaus, U. Hofmann, M. Eichelbaum, M. Schwab and U. M. Zanger, *Pharmacogenetics*, 2001, **11**, 399–415.
26 S. R. Faucette, R. L. Hawke, E. L. Lecluyse, S. S. Shord, B. Yan, R. M. Laethem and C. M. Lindley, *Drug Metab. Dispos.*, 2000, **28**, 1222–1230.
27 J. Hukkanen, M. Mantyla, L. Kangas, P. Wirta, J. Hakkola, P. Paakki, S. Evisalmi, O. Pelkonen and H. Raunio, *BMC Pharmacol. Toxicol.*, 1998, **82**, 93–97.
28 A. Janmohamed, C. T. Dolphin, I. R. Phillips and E. A. Shephard, *Biochem. Pharmacol.*, 2001, **62**, 777–786.
29 T. Thum and J. Borlak, *Lancet*, 2000, **355**, 979–983.
30 V. Lamba, J. Lamba, K. Yasuda, S. Strom, J. Davila, M. L. Hancock, J. D. Fackenthal, P. K. Rogan, B. Ring, A. Wrighton Steven and G. Schuetz Erin, *J. Pharmacol. Exp. Ther.*, 2003, **307**, 906–922.
31 J. Solus, B. J. Arietta, J. R. Harris, D. P. Sexton, J. Q. Steward, C. McMunn, P. Ihrie, J. M. Mehall, T. L. Edwards and E. P. Dawson, *Pharmacogenomics*, 2004, **5**, 895–931.
32 M. Ingelman-Sundberg, S. C. Sim, A. Gomez and C. Rodriguez-Antona, *Pharmacol. Ther.*, 2007, **116**, 496–526.
33 P. Jancova, P. Anzenbacher and E. Anzenbacherova, *Biomedical papers of the Medical Faculty of the University Palacky*, Olomouc, Czechoslovakia, 2010, vol. 154, pp. 103–116.
34 C. Guillemette, *Pharmacogenomics J.*, 2003, **3**, 136–158.
35 A. Mori, Y. Maruo, M. Iwai, H. Sato and Y. Takeuchi, *Drug Metab. Dispos.*, 2005, **33**, 672–675.
36 H. Jinno, M. Saeki, Y. Saito, T. Tanaka-Kagawa, N. Hanioka, K. Sai, N. Kaniwa, M. Ando, K. Shirao, H. Minami, A. Ohtsu, T. Yoshida, N. Saijo, S. Ozawa and J.-I. Sawada, *J. Pharmacol. Exp. Ther.*, 2003, **306**, 688–693.
37 A. Iida, S. Saito, A. Sekine, C. Mishima, Y. Kitamura, K. Kondo, S. Harigae, S. Osawa and Y. Nakamura, *J. Hum. Genet.*, 2002, **47**, 505–510.
38 B. Kuhn, P. Mohr and M. Stahl, *J. Med. Chem.*, 2010, **53**, 2601–2611.
39 C. Sams, G. D. Loizou, J. Cocker and M. S. Lennard, *Toxicol. Lett.*, 2004, **147**, 253–260.
40 Y. Lin, P. Lu, C. Tang, Q. Mei, G. Sandig, A. D. Rodrigues, T. H. Rushmore and M. Shou, *Drug Metab. Dispos.*, 2001, **29**, 368–374.
41 N. Chauret, A. Gauthier and D. A. Nicoll-Griffith, *Drug Metab. Dispos.*, 1998, **26**, 1–4.
42 W. F. Busby Jr, J. M. Ackermann and C. L. Crespi, *Drug Metab. Dispos.*, 1999, **27**, 246–249.
43 L. Oleson and M. H. Court, *J. Pharm. Pharmacol.*, 2008, **60**, 1175–1182.
44 T. Pallmann, PhD thesis, Universität Marburg, 2007.
45 S. Laufer and S. Linsenmaier, *J. Biomol. Screening*, 2006, **11**, 528–536.
46 M. Goettert, R. Graeser and S. A. Laufer, *Anal. Biochem.*, 2010, **406**, 233–234.
47 S. A. Laufer, G. M. Ahrens, S. C. Karcher, J. S. Hering and R. Niess, *J. Med. Chem.*, 2006, **49**, 7912–7915.